JOURNAL OF MATERIALS SCIENCE 35 (2000) 515–520

Fabrication and mechanical properties of α-Al_2O_3/β-Al_2O_3/Al/Si composites by liquid displacement reaction

T. WATARI, T. TORIKAI, W.-P. TAI
Department of Applied Chemistry, Faculty of Science and Engineering, Saga University, Saga 840, Japan
E-mail: watarit@cc.saga-u.ac.jp

O. MATSUDA
Department of Industrial Chemistry, Faculty of Engineering, Tohwa University, Fukuoka 815, Japan

Al_2O_3/metal composites were fabricated by heating three kinds of commercial mullite refractories in contact with Al, and their mechanical properties were investigated. Aluminum reacted with the mullite and SiO_2-glass constituting the mullite refractories and changed them into α-Al_2O_3 and Si. Simultaneously, β-Al_2O_3 was formed by the reactions among α-Al_2O_3 and sodium and potassium oxides in the glassy phase. Also, Al penetrated into the α-Al_2O_3/β-Al_2O_3/Si composite by partly dissolving Si. Finally, the mullite refractories were changed into α-Al_2O_3/β-Al_2O_3/Al/Si composites. The phase contents, microstructures and mechanical properties of the resulting composites varied with the composition of the refractories. The content of β-Al_2O_3 in the composite was lowest at the lowest Na_2O and K_2O contents in the refractories. Silicon in the composite had its highest content at the highest SiO_2 content. The composite fabricated from SiO_2/Al_2O_3 (in mol) (SAR) = 1.85 consisted of 2–5 μm Al_2O_3 grains embedded in metal, but that from SAR = 1.05 showed a complicated microstructure with small and large grains. The bending strength of the composites fabricated from the refractories of SAR = 1.85, 1.24, and 1.05 were 327, 405 and 421 MPa, respectively. Also, the corresponding fracture toughness values were 5.2, 6.1, and 5.5 MPa $m^{1/2}$, respectively.

1. Introduction

Ceramic/metal composites with unique microstructures, layered or aggregated, can be fabricated by the displacement reaction between metal (M) and oxide (A_XO); $yM + A_XO \rightarrow xA + M_yO$ [1–4]. The reaction between solid metal and solid oxide is called the solid displacement reaction. In this system, many combinations of solid metals and oxides have been investigated. For example, the layered structure was observed in the composites prepared with Ni/Cu_2O, Co/Cu_2O and W/Cu_2O systems, and the aggregated was in Fe/Cu_2O, Ti/Cu_2O, Mn/Cu_2O, Nb/Cu_2O and Fe/NiO systems [1, 4]. The occurrence of these unique morphologies was explained by the difference of the rate controlling species in the diffusion process [1], or a side reaction to disturb the interface [4]. In particular, the composite with the latter aggregated microstructure shows promise for improving the mechanical properties of the brittle oxide ceramics as shown in DIMOX^{TM} composites [5].

On the other hand, the liquid displacement reaction between liquid metal and solid oxides has not been thoroughly investigated. The Aluminum/SiO_2 system was studied by reaction kinetics [6], and the resulting Al_2O_3/Al composites showed an aggregated microstructure and had superior mechanical properties [7, 8]. Aluminum and mullite powders were reacted in air to form porous Al_2O_3/Si composites [9]. Recently, dense Al_2O_3/Al/Si composites have been fabricated in Al/mullite systems [10, 11]. In the latter work, mullite bodies with no or slight impurities were reacted with Al in an Ar atmosphere or under low oxygen partial pressure ($\sim 10^{-10}$ atm).

Incidentally, the authors have been investigating the DIMOX^{TM} process using an Al powder compact [12–14] and found that Al metal infiltrated into mullite refractories in air, forming Al_2O_3/metal composites [15]. In this paper, in order to investigate the relation between properties of the resulting composites and the composition of the elemental mullite refractories, three kinds of commercial refractories were used. Also, air atmosphere was adopted for easy processing.

2. Experimental

2.1. Preparation

Three kinds of mullite refractory plates (Nikkato, Tokyo, Japan) with different SiO_2/Al_2O_3 molar ratios

TABLE I Properties of elemental mullite refractories

Sample	Composition (wt %)					SiO_2/Al_2O_3 ratio (in mol)	Bulk density ($g \cdot cm^{-3}$)	Closed pore (vol %)
	SiO_2	Al_2O_3	K_2O	Na_2O	Others*			
HS-R	50.0	46.0	1.9	0.5	1.6	1.85	2.57	11
MS-R	41.0	56.0	1.4	0.5	1.1	1.24	2.68	13
LS-R	37.0	60.0	0.8	0.2	2.0	1.05	2.70	10

*Mainly: Fe_2O_3, CaO, MgO.

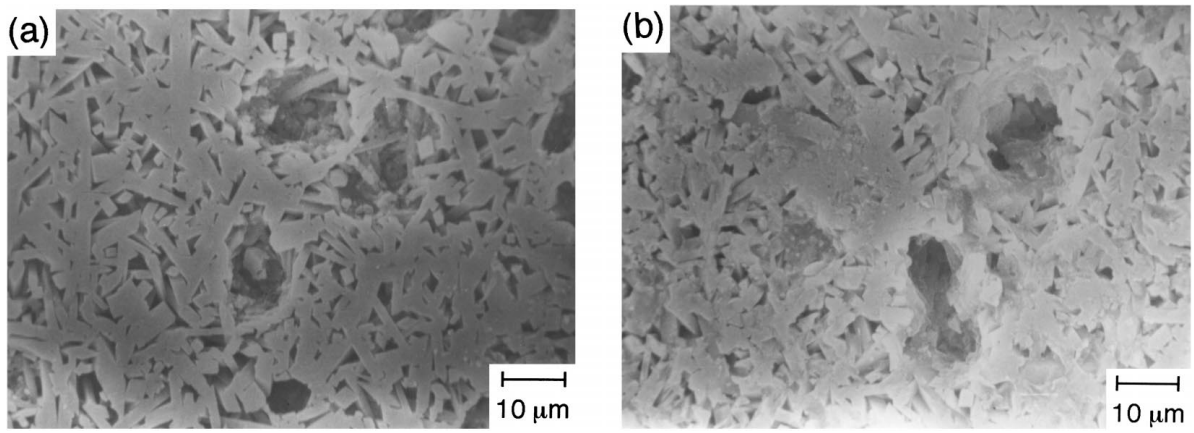

Figure 1 Etched surfaces of unreacted mullite refractories (SiO_2/Al_2O_3 (in mol) = 1.85 (a), 1.05 (b)).

(1.05, 1.24, 1.85) were used as starting materials. These commercial refractories were fabricated from natural aluminosilicate minerals [16]. Table I lists their composition, bulk density, and closed pore volume percentages (no open pores in the refractories). The contents of SiO_2 in all starting materials are higher than that in the stoichiometric mullite (28.2 wt %). The excess silica exists as a glassy state in the refractories. In this report, the elemental refractories consisting of 1.85, 1.24 and 1.05 in a SiO_2/Al_2O_3 molar ratio are named HS-R, MS-R and LS-R, respectively. Fig. 1 shows the microstructures of the mullite crystals in HS-R and LS-R after dissolving the glassy phase with HF solution. HS-R and LS-R have columnar mullite crystals (1–2 μm in width), but HS-R has a wider glass phase between mullite crystals compared to LS-R. MS-R has a similar microstructure to that of LS-R.

A horizontal electric furnace with a refractory tube was used for the reaction. Aluminum powder (0.25 mm, 99.8%, Toyo Aluminum, Ohsaka, Japan) was pressed into bars $10 \times 40 \times 5$ mm at 50 MPa and put on a mullite refractory plate of $12 \times 40 \times 5$ mm in size. After the furnace was heated up to 1000–1200 °C under air flow (l atm), the Al compact with refractory plate was pushed into the hot zone for a few minutes, and then heated for 20 min and 3 h. After that, the furnace was cooled down to room temperature. The products prepared with LS-R, MS-R and HS-R were named LS-C, MS-C and HS-C, respectively, and analyzed by the following technique.

2.2. Evaluation

Thermogravimetry (TG) and a differential thermal analyses (DTA) were carried out using a mixture of Al and HS-R powders. The phases and microstructure of the products were examined by X-ray diffraction (XRD), optical microscope and scanning electron microscope (SEM). The thickness of the resulting composite, which had grown into the refractories, was measured using a traveling microscope. The density of the mullite refractories and the composites was measured by Archimedes' method with water or toluene. The three-point bending test was performed using a specimen of $4 \times 3 \times 40$ mm based on Japan Industrial Standards JIS-R1601. The span length was 30 mm and crosshead speed was 0.5 mm/min. The fracture toughness was evaluated based on the measuring method reported by Yasuda *et al.* [17] using a specimen of $4 \times 3 \times 20$ mm with a chevron notch. A 15-mm span and crosshead speed of 0.05 mm/min were adopted.

3. Results and discussion

3.1. Displacement reaction

Since Al metal is easily oxidized, the reaction between Al and ceramics is usually conducted in an inert atmosphere or under low oxygen pressure. In this work, however, an air atmosphere was used for its convenience. Fig. 2 shows TG-DTA curves on the reaction between Al and HS-R powders under air flow. After melting Al at ~670 °C, the exothermic reaction started at ~760 °C and four peaks were observed. Simultaneously, the weight gain due to the oxidation of Al occurred. Since it is understandable on the basis of TG-DTA curves that the reaction occurred up to 1000 °C, the fabrication of the composite was examined above 1000 °C in order to complete the reactions. The color of the mullite refractories changed from white to dark gray after the reaction, then the thickness of the reacted zone could be measured using a traveling microscope. The thickness of the product increased with increasing

temperatures; 0.4 mm at 1000 °C, 2.0 mm at 1100 °C and 2.7 mm at 1200 °C on reacting HS-R with Al for 20 min. The growth rate of the product decreased with time (Fig. 3). This behavior is similar to that reported by Loehman *et al.* [10], but the growth rate of this work is almost half of that of the report. This must be due to the difference of the contacted area between the Al and mullite plates. In the report [10], Al drop was used and the reaction was conducted under an Ar atmosphere, therefore, a good contact between Al and mullite plates was achieved. On the other hand, the Al powder compact and air atmosphere in this work restricted the contact area between Al and mullite plates. The limited contact was observed by an optical microscope.

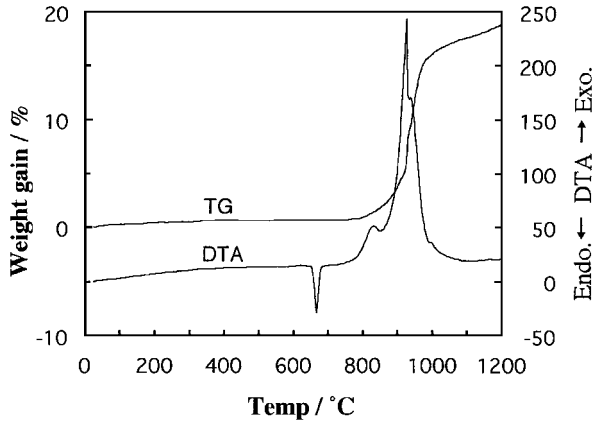

Figure 2 TG-DTA curves of mixed powder of Al and mullite refractories (SiO_2/Al_2O_3 (in mol) = 1.85).

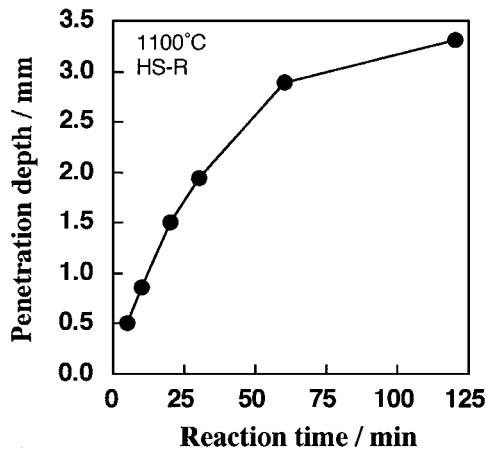

Figure 3 Penetration depth of Al into mullite refractories (SiO_2/Al_2O_3 (in mol) = 1.85) at 1100 °C as a function of reaction time.

Hereafter, the reaction was conducted at 1150 °C for 3 h. After processing, the shape of the Al compact did not change owing to the protective oxide film covering each Al particle in the air atmosphere. Aluminum metal, however, interconnected through the compact and was supplied to the reaction zone. The XRD pattern of the product with HS-R is depicted in Fig. 4. Mullite, the only crystal phase in the elemental refractories, disappeared and changed into Al_2O_3 and Si in the same manner as other works [10, 11].

$$3(3Al_2O_3{\cdot}2SiO_2)(s) + 8Al(l) \rightarrow 13Al_2O_3(s) + 6Si(s) \quad (1)$$

Furthermore, the reports on the Al/SiO_2 reaction [6–8] suggest that in the present work, the glassy SiO_2 surrounding mullite crystals also reacted with Al as in the following equation, although it can not be judged from XRD measurements.

$$3SiO_2(s) + 4Al(l) \rightarrow 2Al_2O_3(s) + 3Si(s) \quad (2)$$

Moreover, a β-Al_2O_3 type phase was detected in the products. Hirata *et al.* reported the formation of β-Al_2O_3 by heating Na_2O-containing Al_2O_3 compacts [18]. In the present work, the components such as sodium and potassium oxides in the glassy phase should react with Al_2O_3, which was formed according to Equations 1 and 2, and form β-Al_2O_3 as follows.

$$R_2O(R; Na^+, K^+)(s) + 11Al_2O_3(s) \rightarrow R_2O{\cdot}11Al_2O_3(s) \quad (3)$$

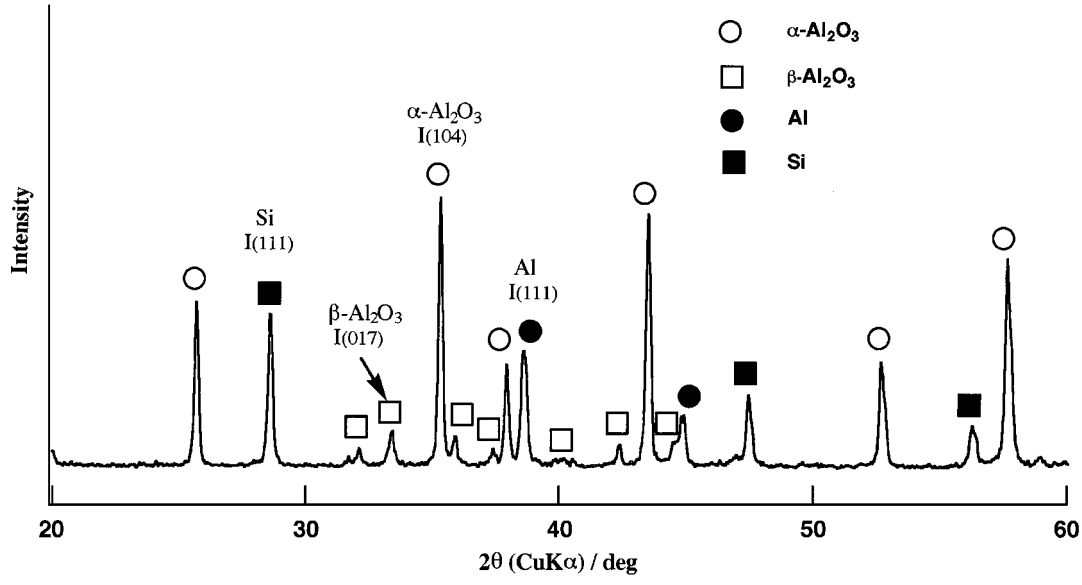

Figure 4 XRD pattern of composite fabricated from refractories of SiO_2/Al_2O_3 (in mol) = 1.85.

Although Equations 1–3 do not show an Al phase in the product, the resulting composite contained Al metal (Fig. 4). It means that Si, which was formed according to Equations 1 and 2, was displaced with molten Al [11].

The content of each phase in the product varied with the composition of the elemental refractories. Fig. 4 shows the change in content of each phase with the SiO_2/Al_2O_3 molar ratios of the refractories. In Fig. 5, the fraction of each phase, f(phase), was represented by the ratios of X-ray diffraction intensity of Al_2O_3(104), β-Al_2O_3(017), Al(111) and Si(111), whose peaks are shown in Fig. 4. The $f(Al_2O_3)$ was almost independent of the SiO_2/Al_2O_3 ratio, but f(Al) decreased at $SiO_2/Al_2O_3 = 1.85$ and, vice versa, f(Si) increased. This increase of Si content is explained by the relatively high content of SiO_2 in the elemental refractories. In the composite from $SiO_2/Al_2O_3 = 1.05$, the content of $f(\beta\text{-}Al_2O_3)$ was low due to the small amount of Na_2O and K_2O in the elemental refractories as listed in Table I. The calculated amounts of β-Al_2O_3 are 27.0 vol % (26.3 wt %) for HS-C, and 12.7 vol % (11.8 wt %) for LS-C, on the basis of Equation 3 and the composition of refractories (Table I) under the assumption of no penetration of Al. The calculated contents of β-Al_2O_3 are relatively large.

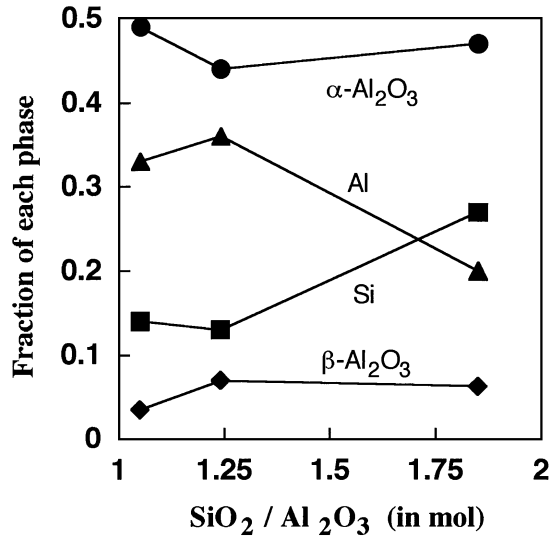

Figure 5 Fraction of each phase in resulting composites as a function of SiO_2/Al_2O_3 molar ratio. (Phase fraction $= I_{phase}(hkl)/\{I_{\alpha-Al_2O_3}(104) + I_{\beta-Al_2O_3}(017) + I_{Al}(111) + I_{Si}(111)\}$).

The optical micrographs of the composites, HS-C and LS-C, are shown in Fig. 6a and b, respectively. The microstructure of MS-C is similar to that of LS-C. The dark area in the picture corresponds to α-Al_2O_3 and β-Al_2O_3 phases, and their grains are interconnected in the composites. The bright area represents Al and Si, and they are also continuous through the composite because the composite showed electrical conductivity. The microstructure changed by the SiO_2/Al_2O_3 ratio of elemental refractories. The HS-C has Al_2O_3 grains of 2–5 μm in size, but the LS-C has smaller grains and metal phases among larger grains. These microstructures seem to be closely related to the ones of elemental refractories (Fig. 1).

The bulk and true densities of HS-C are 3.30 and 3.34 g cm^{-3}, those of MS-C are 3.20 and 3.42 g cm^{-3}, and those of LS-C are 3.44 and 3.78 g cm^{-3}, respectively. Then, the porosities of HS-C, MS-C and LS-C are calculated as 1, 6 and 9 vol %, respectively. The elemental refractories are of almost the same porosity, 10 to 13 vol %, but those of the composite decreased with an increasing SiO_2/Al_2O_3 ratio in the refractories.

Gao *et al.* [19] found that, in the reactive infiltration process with mullite bodies and Al, Al penetrated at first through the grain boundaries and then to the mullite crystals. In the present work, the elemental refractories have a glassy phase around the mullite crystals (Fig. 1). Therefore, the penetration according to Equation 2 should also be considered. To understand the macroscopic penetration phenomenon, the advancing composite into the HS-R was observed with an optical microscope (Fig. 7). A gray boundary of $\sim$20 μm in width is located between the refractories and the composite (Fig. 7a). Fig. 7b shows no trace of preferential penetration in the advancing area as shown in the DIMOX^{TM} process [13]. The reactions of Equations 1 and 2 seem to occur simultaneously. These pictures show that the gray boundary beside the composite was invaded by metal and separated into small grains. The boundary penetration of Al [19] may also occur in this work. Closed pores still exist in the boundary, but disappear just inside the composite. If the disappearance of pores occurred by the infiltration of molten metal,

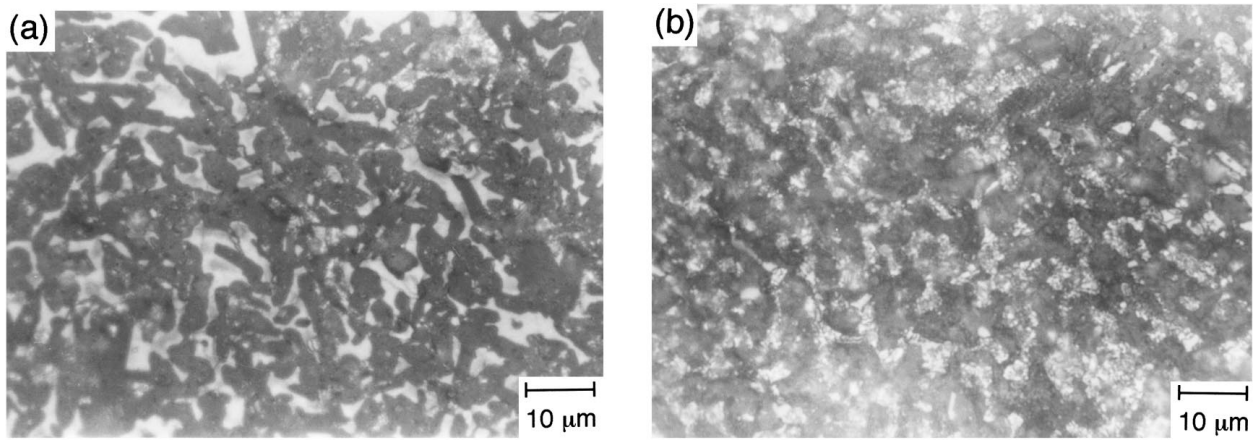

Figure 6 Optical micrographs of α-Al_2O_3/β-Al_2O_3/Al/Si composites (SiO_2/Al_2O_3 (in mol) of elemental refractories = 1.85 (a), 1.05 (b)).

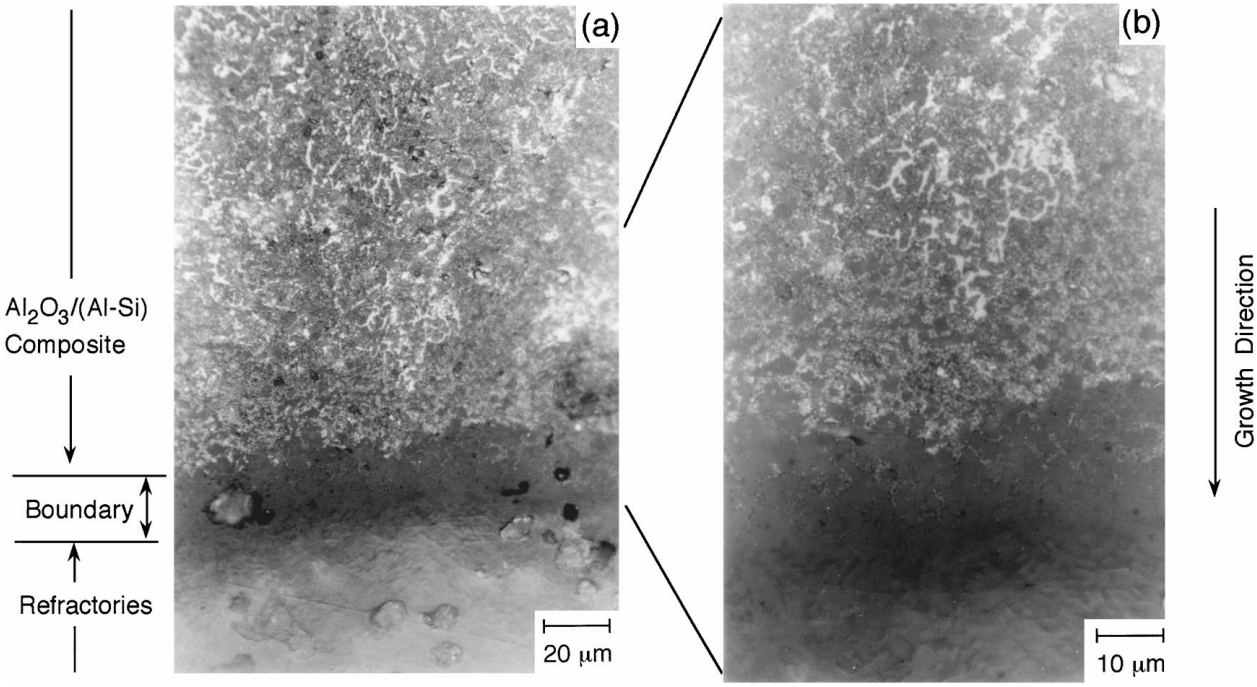

Figure 7 Optical micrographs of the front of advancing composite into refractories of SiO_2/Al_2O_3 (in mol) = 1.85.

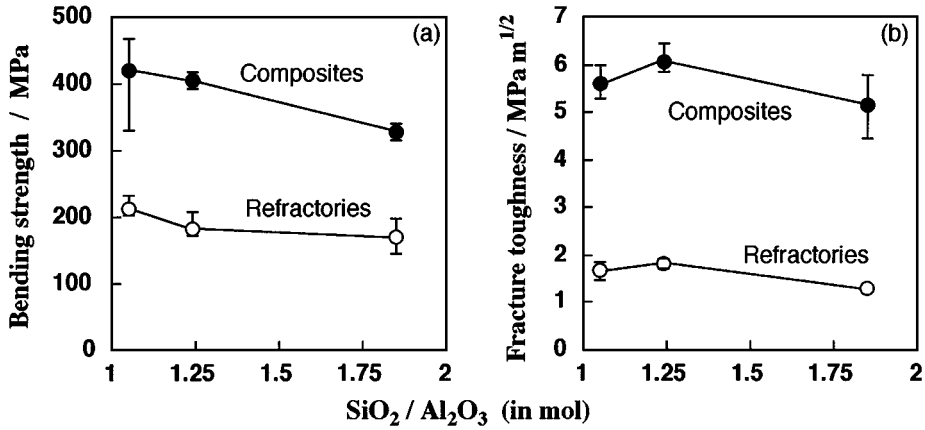

Figure 8 Bending strength and fracture toughness of elemental refractories and α-Al_2O_3/β-Al_2O_3/Al/Si composites as a function of SiO_2/Al_2O_3 molar ratio.

some metal phases of the same shape and size as the pores should exist in the resulting composite. The size of the metal phase is smaller than that of the pores (3–10 μm). Therefore, by filling the pores, some reactions should occur.

3.2. Mechanical properties

The resulting composites fabricated by liquid displacement reactions have mechanical properties superior to the raw refractories as shown in Fig. 8a and b. In these figures, the properties of the composites are plotted as a function of the SiO_2/Al_2O_3 molar ratios of the elemental refractories. The bending strengths of the refractories, HS-R, MS-R and LS-R, are 170, 183 and 212 MPa, respectively. These values are lower than those of the sintered mullite body using a sol-gel stoichiometric powder [20]. This must be due to the glassy phase and pores in the refractories. The liquid displacement reaction increased the strength up to 327 MPa (HS-C), 405 MPa (MS-C) and 421 MPa (HS-C) as shown in Fig. 8a. The disappearance of silica glass may increase the strength. The strength of the composites increased with a decreasing SiO_2/Al_2O_3 ratio, even though their porosities increased. The fracture toughness also increased from 1.3 MPa m$^{1/2}$ (HS-R), 1.8 MPa m$^{1/2}$ (MS-R) and 1.7 MPa m$^{1/2}$ (LS-R) to 5.2 MPa m$^{1/2}$ (HS-C), 6.1 MPa m$^{1/2}$ (MS-C) and 5.6 MPa m$^{1/2}$ (LS-C). The reason for this large increase in toughness can be seen from a comparison of the fracture surfaces between MS-R (Fig. 9a) and MS-C (Fig. 9b) after a mechanical test. The composites show many projection-like ridges, which are visible as bright lines in the pictures, and some basins resulted from the pull-out grains, but the refractories have a relatively smooth surface. This type of projection was observed on the fracture surface of the Al_2O_3/Al-alloy composites fabricated by the DIMOX^{TM} process [21, 22], showing a stretching Al ligament embedded in an alumina matrix. Here, it can be supposed that this plastic stretch inhibited cracks

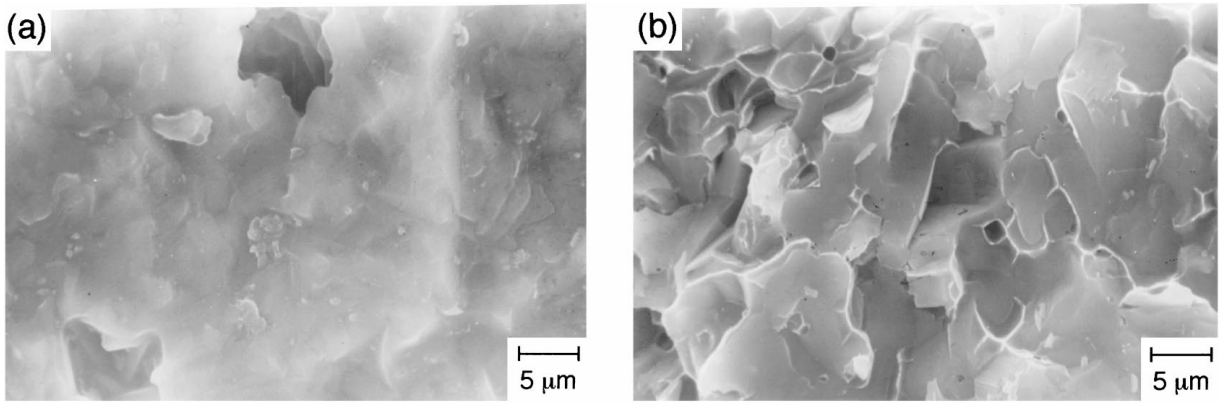

Figure 9 Fracture surfaces of elemental refractories (a) (SiO_2/Al_2O_3 (in mol) = 1.85) and resulting α-Al_2O_3/β-Al_2O_3/Al/Si composite (b).

and resulted in the increase of fracture toughness of the composite. The change in fracture toughness of the composite with the SiO_2/Al_2O_3 ratio agrees with that of the Al content in the composites (Fig. 5).

The bending strength of the α-Al_2O_3/β-Al_2O_3/Al/Si composite is close to that of the composite fabricated by the liquid displacement reaction between SiO_2 and Al [7]. The fracture toughness of the composite in this work, however, is almost half of that of the report. This must be that the composites fabricated from an SiO_2/Al system have a higher amount of Al (30 wt %) without Si. Therefore, the fracture toughness of the composite in this work may be increased more by the displacement of Si with Al by any process, e.g., by dipping the composite into a molten Al bath.

4. Conclusion

Using the liquid displacement reaction between commercial mullite refractories and Al metal, α-Al_2O_3/β-Al_2O_3/Al/Si composites with improved mechanical properties can be fabricated.

1. Aluminum reacted with the mullite refractories and changed them into α-Al_2O_3, β-Al_2O_3 and Si. Then, Al penetrated into the α-Al_2O_3/β-Al_2O_3/Si composite by displacing Si.

2. The content of β-Al_2O_3 in the composite was lowest at the lowest Na_2O and K_2O contents in the refractories. Silicon in the composite had its highest content at the highest SiO_2 content in the refractories. The composite fabricated from SiO_2/Al_2O_3 (in mol) = 1.85 consisted of 2–5 μm Al_2O_3 grains embedded in metal.

3. The bending strengths of the composites were from 327 to 421 MPa, and the fracture toughness values were from 5.2 to 6.1 MPa $m^{1/2}$.

Acknowledgement

The authors are grateful for discussions with and the supply of reprints by Professor Yoshihiro Hirata. The authors also wish to thank Mr. Kuwata at Saga Ceramics Research Laboratory for TG-DTA measurement. This work was supported by Ministry of Education, Culture and Science with a subsidy (A) (No. 05750617) of the Science and Research Fund, and by Nippon Sheet Glass Foundation for Materials Science and Engineering. One of the authors (W. P. Tai) would also like to thank Korea Science and Engineering Foundation for its financial support.

References

1. R. A. RAPP, A. EZIS and G. J. YUREK, *Metall. Trans.* **4** (1973) 1283.
2. F. J. J. VAN LOO, J. A. VAN BEEK, G. F. BASTIN and R. METSELAAR, *Oxid. Metals* **22** (1984) 161.
3. H. TAIMATSU, S. SUZUKI, M. KITANO and H. KANEKO, *J. Ceram. Soc. Jpn.* **102** (1994) 170.
4. H. TAIMATSU, Y. IKEDA, N. NEMOTO, T. KIMURA and H. KANEKO, *Z. Metallkde* **81** (1990) 588.
5. M. K. AGHAJANIAN, N. H. MACMILLAN, C. R. KENNEDY, S. J. LUSZCZ and R. ROY, *J. Mater. Sci.* **24** (1989) 658.
6. A. E. STANDAGE and M. S. GANI, *J. Amer. Ceram. Soc.* **50** (1967) 101.
7. M. C. BRESLIN, J. RINGNALDA, J. SEEGER, A. L. MARASCO, G. S. DAEHN and H. L. FRASER, *Ceram. Eng. Sci. Proc.* **15** (1994) 104.
8. S. MATSUO and T. INABA, *Seramikkusu* **26** (1991) 222.
9. M. IMAMURA, K. NAKAJIMA, A. YANAGISAWA and T. NAKAGAWA, *Funtai Oyobi Funmatsu Yakin* **40** (1993) 516.
10. R. E. LOEHMAN, K. EWSUK and A. P. TOMSIA, *J. Amer. Ceram. Soc.* **79** (1996) 27.
11. E. SAIZ, A. P. TOMSIA, R. E. LOEHMAN and K. EWSUK, *J. Eur. Ceram. Soc.* **16** (1996) 275.
12. T. WATARI, K. OHTA, N. OHTA, T. TORIKAI and O. MATSUDA, *J. Ceram. Soc. Jpn.* **100** (1992) 1405.
13. T. WATARI, K. MORI, T. TORIKAI and O. MATSUDA, *J. Amer. Ceram. Soc.* **77** (1994) 2599.
14. T. WATARI, K. INOUE, T. TORIKAI and O. MATSUDA, *Ceram. Trans.* **51** (1995) 225.
15. T. WATARI, H. KOBAYASHI, T. TORIKAI, W.-P. TAI and O. MATSUDA, in Proceedings of Annual Meeting of Ceramic Society of Japan, Tokyo, April 1995, p. 525.
16. T. KAWANAMI, in "Mullite," edited by S. Somiya (Uchida Rokakuho Publishing Co., Tokyo, Japan, 1985) p. 123.
17. E. YASUDA, T. AKATSU and Y. TANABE, *J. Ceram. Soc. Jpn.* **99** (1991) 52.
18. Y. HIRATA, T. IZAIKU and Y. ISHIHARA, *J. Mater. Res.* **6** (1991) 585.
19. Y. GAO, J. JIA, R. E. LOEHMAN and K. G. EWSUK, *ibid.* **10** (1995) 1216.
20. H. OHNISHI, T. KAWANAMI, A. NAKAHIRA and K. NIIHARA, *J. Ceram. Soc. Jpn.* **98** (1990) 541.
21. L. S. SIGL, P. A. MATAGA, B. J. DALGLEISH, R. M. MCMEEKING and A. G. EVANS, *Acta Metall.* **36** (1988) 945.
22. C. A. ANDERSSON and M. K. AGHAJANIAN, *Ceram. Eng. Sci. Proc.* **9** (1988) 621.

Received 24 June 1996
and accepted 20 July 1999